Ⅲ-5

Life, Earth and Planetary Sciences

BL1U

Optical Activity Emergence in Amino-Acid Films by Vacuum-Ultraviolet Circularly-Polarized Light Irradiation (I) - Experimental Setup -

J. Takahashi[1], K. Matsuo[2], Y. Izumi[2], K. Kobayashi[1], M. Fujimoto[3] and M. Katoh[3]
[1]*Fucalty of Engineering, Yokohama National University, Yokohama 250-8501, Japan*
[2]*Hiroshima Synchrotron Radiation Center, Higashi-Hiroshima 739-0046, Japan*
[3]*UVSOR Synchrotron Facility, Institute for Molecular Science, Okazaki 444-8585, Japan*

The origin of homochirality in terrestrial bioorganic compounds (dominant L-amino acid and D-sugar) is one of the most mysterious issues that remain unresolved in the study of the origin of life. Because bioorganic compounds synthesized in abiotic circumstances are intrinsically racemic mixtures of equal amounts of L- and D-bodies, it is hypothesized that chiral products originated from asymmetric chemical reactions. These types of asymmetric reactions could have possibly been derived from physically asymmetric excitation sources in space, that is "chiral radiation", and the chiral products would have been transported to primitive Earth resulting in terrestrial biological homochirality (Cosmic Scenario) [1]. Eventually, terrestrial observations of circularly-polarized light (CPL) radiation due to scattering by interstellar dust clouds in star formation regions have been reported [2].

Several ground experiments have already examined asymmetric photochemical reactions in simple biochemical molecules by CPL. We reported optical activity emergence in solid-phase films of racemic mixtures of amino acids by CPL irradiation of 215 nm in wavelength from free electron laser (FEL) of UVSOR-II [3].

Recently, we are carrying out the measurement of CPL irradiation wavelength dependence of optical activity emergence by tuning undurator gap conditions. We have already also reported the optical activity emergence by using CPL irradiation of 230, 215, and 203 nm in wavelength from undulator BL1U of UVSOR-III [4].

Presently, we are trying to introduce optical activity by vacuum ultraviolet (VUV) CPL irradiation in shorter wavelength than 200 nm . As for the sample, we formed thin solid films of racemic DL-alanine on fused quartz substrates using a thermal-crucible vacuum evaporator from crystal powders of DL-alanine as a sublimation source. Sublimation temperature was in the range of 150~200°C and pressure of the vacuum chamber was approximately 10^{-2} Pa throughout the evaporation process. In order to introduce optical activity into the racemic film, we irradiate them with CPL introduced from undulator BL1U of UVSOR-III. The samples were set in a vacuum sample chamber preventing VUV CPL attenuation by air absorption in shorter wavelength than 200 nm (Fig.1). On the beam entrance side of the vacuum sample chamber, a gate valve with a vacuum-sealed MgF_2 window was mounted. The irradiated CPL wavelengths were 180, 155, and 120 nm corresponding to photon absorption bands of alanine molecule. The irradiated photon number was measured with photoelectron current of a silicon photodiode (International Radiation Detectors, Inc.) settled at the sample position. The typical energy dose calibrated by quantum efficiency of the silicon photodiode was approximately 50mWhour.

In order to clarify the optical anisotropy of the films before and after VUV CPL irradiation, we measured the synchrotron radiation (SR) circular dichroism (CD) at beamline BL-12 of Hiroshima Synchrotron Radiation Center (HiSOR). In order to delete the effects of linear dichroism (LD) and/or linear birefringence (LB) components, dependence on sample rotation angle (0, 45, 90, and 135degrees) of the CD spectra was measured.

Through the VUV CPL irradiation experiments and the detailed analysis of SR-CD spectra, we are aiming to clarify full mechanism of the optical activity emergence, which potentially has relevance to the origin of terrestrial biological homochirality.

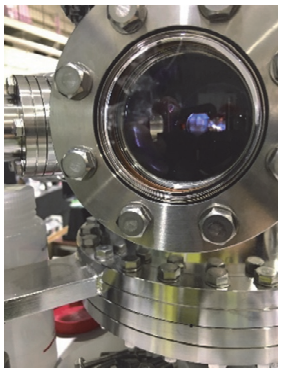

Fig. 1. Photo of VUV CPL irradiation experiment on BL1U using a vacuum sample chamber.

[1] W. A. Bonner, Orig. Life Evol. Biosph. **21** (1991) 59.
[2] T. Fukue *et al.*, Orig. Life Evol. Biosph. **40** (2010) 335.
[3] J. Takahashi *et al.*, Int. J. Mol. Sci. **10** (2009) 3044.
[4] K. Matsuo *et al.*, UVSOR Activity Report **44** (2017) 157.

BL1B, BL7B

Giant Thermal Effect of Vibration Modes of Single-Crystalline Alanine

Z. Mita[1], H. Watanabe[1, 2] and S. Kimura[1, 2]

[1] *Graduate School of Frontier Biosciences, Osaka University, Suita, 565-0871, Japan*

[2] *Department of Physics, Graduate School of Science, Osaka University, Toyonaka, 560-0043, Japan*

Amino acids are the most basic molecules of living bodies. Since almost all amino acids are chiral materials, they have enantiomers, L- and D-form. Although amino acids are well-known, fundamental physical properties have hardly been studied. Owing to the crystal structure, strong anisotropy of optical constants and ferroelectricity are expected. However, the optical measurements using single-crystalline samples have never been studied so far, neither the temperature dependence. Here we report the temperature-dependent anisotropic reflectivity spectra of single-crystalline L-alanine that has the simplest molecular structure among amino acids having chirality.

We have grown the single crystal by using the solvent evaporation method and confirmed to be orthorhombic structure reported previously [1]. Polarized optical spectra from the terahertz (THz) to vacuum-ultraviolet (VUV) regions have been measured by using BL1B [2] and BL7B [3] at UVSOR-III and laboratorial equipments. Temperature dependence of anisotropic reflectivity spectra in the THz region are shown in Fig. 1. Some peaks owing to molecular vibrations appear. The optical spectra are strongly anisotropic and all of these peaks have large temperature dependency. For instance, the intensity of the peak appearing at the photon energy of about 15 meV (indicated by a red square in Fig. 1) in the configuration of the electric vector parallel to the *c*-axis (*E* // *c*) increases 4 times larger with decreasing temperature from 300 K to 10 K. The obtained reflectivity spectra were converted to the optical conductivity spectra by using the Kramers-Kronig analysis. The temperature-dependent peak at 15 meV is shown in Fig. 2.

To explain the temperature dependence, we adopt the Morse potential that is one of the simplified potentials having anharmonicity [4]. Here, we assume the Boltzmann distribution for oscillators' occupation. Assuming the multiple excitation among energy levels, the temperature dependence of the peak in Fig. 2 can be reproduced by using the summation of Lorentz functions owing to the excitations. The results reproduce well as shown by thin lines in Fig. 2. Furthermore, using the parameters obtained from the simulation, the bottom energy of the Morse potential can be evaluated as 822 meV at 10 K and 675 meV at 300 K. The change of the potential shape is the origin of the giant thermal effect of the molecular vibrations of single-crystalline L-alanine.

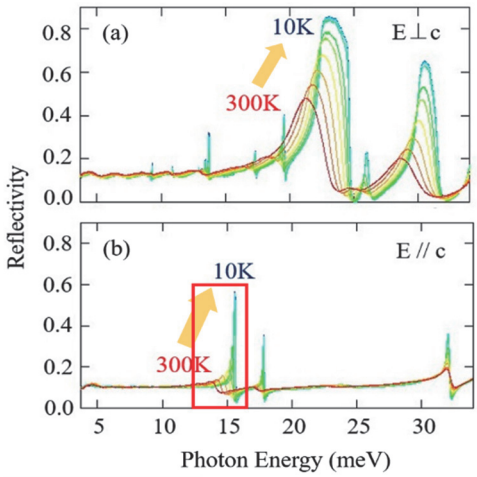

Fig. 1. Anisotropic reflectivity spectra at temperatures from 10 to 300 K in THz regions perpendicular (a) and parallel (b) to the c-axis.

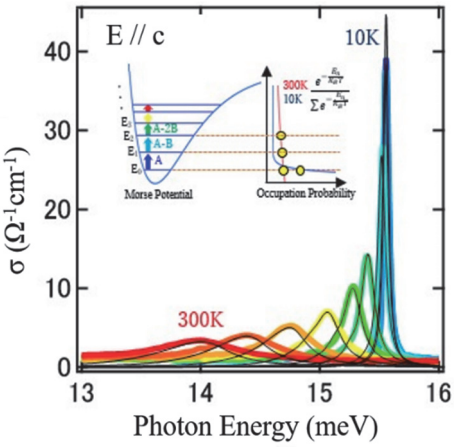

Fig. 2. Temperature-dependent optical conductivity [σ(ω)] spectra of the 15meV peak (thick lines). Thin lines are the simulation results using a simplified anharmonic Morse potential.

[1] M. Fleck and A. M. Petrosyan, Salts of Amino Acids-Crystallization Structure and Properties (Springer, 2014) p. 26.
[2] S. Kimura, E. Nakamura, K. Imura, M. Hosaka, T. Takahashi, M. Katoh, J. Phys.: Conf. Ser. **359** (2012) 012009.
[3] K. Fukui, H.Miura, H. Nakagawa, I. Shimoyama, K. Nakagawa, H. Okamura, T. Nanba, M. Hasumoto, T. Kinoshita, Nucl. Instrum. Meth. Phys. Res. A **467-468** (2001) 601.
[4] P. M. Morse, Phys. Rev. **34** (1929) 57.

BL3U

Novel Insights to Cloud Water Microphysics Using Synchrotron-excited XAS

J. J. Lin[1], G. Michailoudi[1], H. Yuzawa[2], H. Iwayama[2, 3], M. Nagasaka[2, 3], M. Huttula[1], N. Kosugi[2, 3] and N. L. Prisle[1]

[1]*Nano and Molecular Systems Research Unit, University of Oulu, Oulu 90041, Finland*
[2]*UVSOR Synchrotron Facility, Institute for Molecular Science, Okazaki 444-8585, Japan*
[3]*School of Physical Sciences, The Graduate University for Advanced Studies (SOKENDAI), Okazaki 444-8585, Japan*

Cloud droplets in the atmosphere are complex aqueous mixtures of organic and inorganic constituents, but their exact composition and the nature of aqueous phase molecular interactions are extremely challenging to quantify [1]. Amphiphilic compounds present in the organic aerosol fraction are known to self assemble into micelles, but direct chemical information on the aqueous phase interactions of amphiphilic monomers and their aggregate structures has been lacking.

Two types of samples were analyzed with synchrotron radiation X-ray absorption spectroscopy using the liquid cell setup at BL3U [2]: 1) cloud water collected from October 10-14 at the Finnish Meteorological Institute Pallas-Sodankylä Global Atmosphere Watch station in the sub-Arctic region in Finnish Lapland as part of the 7th Pallas Cloud Experiment from September 1 to November 30; and 2) organic micellar systems composed of n-octanoic acid, n-decanoic acid, and sodium n-decanoate dissolved in water at varying multiples of their critical micelle concentration (CMC). A summary of the samples measured is given in Table 1.

For the cloud water samples, both the oxygen K-edge in the 528-550 eV range and the carbon K-edge in the 280-300 eV range were studied. Unfortunately, due to the apparently very low concentration of organic material in the cloud water, presumably from very clean Arctic conditions, any difference between cloud water spectra and pure water spectra could not be detected. Another batch of the cloud water sample will be subject to various complementary analyses to confirm this.

For the aqueous organic micellar solutions, the carbon K-edge in the 280-300 eV range was studied. Photon energies in the 280-285 and 290-300 eV range were scanned at 0.1 eV resolution while photon energies in the 285-290 eV range were scanned at 0.02 eV resolution in order to specifically capture the aliphatic R(CH)R' and carboxylic C(=O)OH carbon absorption peaks from monomers to identify shifts in peak location due to the difference in chemical environment between monomers and micelles in solution.

Preliminary absorption spectra at the C 1s absorption edge for sodium n-octanoate in water at various concentrations along with pure octanoic acid are shown in Fig. 1. Background absorption due to water and the cell membranes have been removed. For all the samples, one main peak is observed at around 289 eV. For sodium n-octanoate solution below the CMC, the absorption spectra before and after the main feature are less than those solutions above the CMC. Interestingly, the higher the sodium n-octanoate concentration in solution, the more the absorption spectra start to resemble that of pure octanoic acid. The measurements hold promise for detecting the aqueous-phase interactions of organic monomer and micellar structures compounds in solution.

Table 1. Summary of samples measured

Sample	CMC [mM]	Concentrations	Number of scans
Cloud Water	–	–	5
n-octanoic acid	140. [3]	0.75, 1.25, 2, 3, 4, 6, and 8 times CMC; pure	15
Sodium n-octanoate	340.0 [4]	0.75, 2, 3, 4, and 5 times CMC	7
Sodium n-decanoate	94.0 [4]	2, 3, 4, 6, and 8 times CMC	10

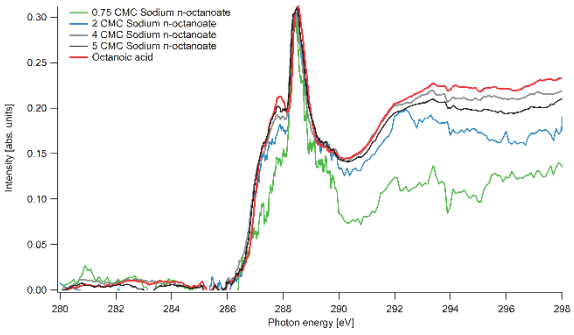

Fig. 1. Preliminary absorption spectra for sodium n-octanoate solutions at various concentrations together with that of pure octanoic acid.

[1] T. Kurtén *et al.*, J. Phys. Chem. A **119** (2014) 4509.
[2] M. Nagasaka *et al.*, J. Electron Spectrosc. **177** (2010) 130.
[3]A. N. Campbell and G. R. Lakshminarayanan, Can. J. Chem. **43** (1965) 1729.
[4] K. Quast, Miner. Eng. **19** (2010) 582.

BL4U

Feasibility Study of Sulfur Speciation High-spatial Resolution Mapping in Extraterrestrial Organics by STXM-XANES

M. Ito[1], R. Nakada[1], H. Suga[2], T. Ohigashi[3], Y. Kodama[4] and H. Naraoka[5]

[1] *Kochi inst. for Core Sample Res., JAMSTEC, Nankoku 783-8502, Japan*

[2] *Hiroshima University, Higashihiroshima 739-0046, Japan*

[3] *UVSOR Synchrotron Facility, Institute for Molecular Science, Okazaki 444-8585, Japan*

[4] *Marine Works Japan LTD., Japan*

[5] *Kyushu University, Fukuoka 819-0395, Japan*

Sulfur is one of the major elements in terrestrial and extraterrestrial organics. The elemental compositions of the Murchison IOM (insoluble organic matter) are proposed to be $C_{100}H_{70}O_{22}N_3S_7$ [1] or $C_{100}H_{48}N_{1.8}O_{12}S_2$ [2]. Because sulfur shows a wide range in oxidation state (-2 to +6) with both electropositive and electronegative elements, reduced and oxidized sulfur species have been found in various carbonaceous chondrites [3, 4]. Therefore, understanding of speciation of sulfur and its distribution within organics in a carbonaceous chondrite may provide the secondary alteration processes of thermal metamorphism and aqueous alteration in the parent body.

Synchrotron based X-ray absorption near edge spectroscopy (XANES) is a powerful analytical tool to characterize and quantify chemical speciation, functional group and bonding environment of the sample. In the field of cosmochemistry, many researches were carried out to identify functional groups of C, N and O in extraterrestrial organics (i.e., IOM in carbonaceous chondrites [5], cometary returned sample [6], organics found in Hayabusa Category-3 particles [7], organics in IDPs [8], and organic component extracted from halite grain in Monahans LL chondrite [9]). However, sulfur study using XANES in the extraterrestrial organics is very rare [3, 10].

In this study, we report preliminary results of sulfur speciation measurements by L_3-edge XANES of series sulfur bearing terrestrial organics to obtain reference spectra, and of S, N, C and O-XANES in the FIB section of the Murchion CM2 carbonaceous chondrite (147 x 187 pixels, 22 x 28 μm^2: spatial resolution = 150 nm) using scanning transmission X-ray microscope (STXM) at Inst. Mole Sci. UVSOR BL4U. We also took a sulfur image (L_3-edge XANES) of organics extracted from Asuka881458 CM2 chondrite for comparison in terms of sulfur distribution and speciation.

We show nine reference sulfur L_3-edge spectra measured by the STXM. Reference sulfur bearing organics are sodium lauryl sulfate, sodium methanesulfonate, dibenzothiophene, thianthrene, DL-methionie, DL-methionine sulfone, L-cysteic acid, L-cystein, and L-cystine (Fig. 1). These organics show different absorption curves which related to sulfur related chemical bond (e.g., sulfate, sulfone, thiol).

We successfully obtained high resolution sulfur STEXM images of both FIB sections of Murchison and organics from Asuka881458. We will continue to measure another primitive chondrite for understanding of diversity of organics based on sulfur speciation. We plan to combine sulfur isotope imaging with NanoSIMS for same sections that used in this study.

[1] L. Remusat, EPJ Web of Conferences **18** (2011) 05002.
[2] Gilmour, Meteorites, Comets, and Planets, Treatise on Geochemistry (2005) 269.
[3] Orthous-Daunay *et al*., EPSL **300** (2010) 321.
[4] W. J. Cooper *et al*., Science **277** (1997) 1072.
[5] G. D. Cody *et al*., Meteor Planet Sci. **43** (2011) 353.
[6] S. A. Sanford *et al*., Science **314** (2006) 1720.
[7] H. Yabuta *et al*., EPS **66** (2014) 156.
[8] G. J. Flynn *et al*., Geochim Cosmochim Acta **67** (2003) 4791.
[9] Chan *et al*., Science Advance **4** (2018) eaao3521.
[10] M. Bose *et al*., Meteor Planet Sci. **52** (2017) 546.

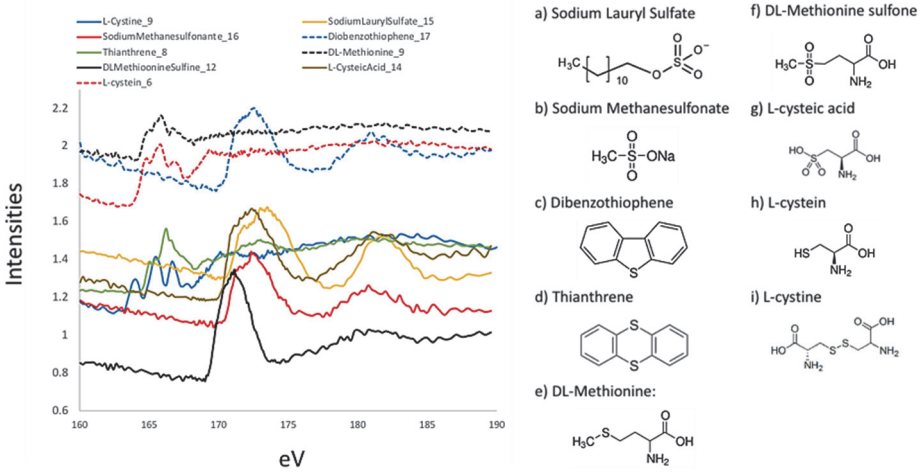

Fig. 1. Sulfur bearing organics of L_3-edge STXM-XANES spectrum

BL4U

Organic Vein in a Primitive Clast in the Carancas Meteorites

Y. Kebukawa[1], M. E. Zolensky[2], T. Ohigashi[3] and Y. Inagaki[3]
[1]*Faculty of Engineering, Yokohama National University, Yokohama 240-8501, Japan*
[2]*ARES, NASA Johnson Space Center, Houston, TX 77058, USA*
[3]*UVSOR Synchrotron Facility, Institute for Molecular Science, Okazaki 444-8585, Japan*

Primitive xenolithic clasts are often found in various groups of meteorites [e.g., 1, 2]. These xenoliths sometime contain unique carbonaceous matter. We have been analyzed these using scanning transmission X-ray microscopes (STXM) combined with other microscopic techniques [3-5]. Some of these could be candidates of primordial trans- Neptunian object (TNOs) that have been scattered by giant planetary migration. It was suggested that numerous bodies was injected from outer Solar System into the main asteroid belt, where modeling shows they can successfully reproduce the observed D/P-type asteroid populations [e.g., 6]. After implantation, some of the D/P-asteroids would have collided with parent body(s) of ordinary chondrites (S-type asteroids). Some of the fragments from D/P-asteroids left in the ordinary chondrite parent body(s) and eventually could be delivered to Earth as meteorites [7]. The Carancas meteorite is a H4-5 ordinary chondrite that contains a primitive xenolithic clast rich in organic matter.

We are conducting coordinated analysis of organic matter in the clast using various methods [8]. 100 nm-thick FIB sections were prepared from the clast using a Quanta 3d field-emission gun FIB instrument at NASA JSC. We investigated the FIB sections with C,N,O-X-ray absorption near-edge structure (XANES) using the STXM at BL4U of UVSOR.

Figure 1 shows a carbon map containing ~10 μm C-rich vein in the clast from Carancas meteorite. C-XANES spectrum of the C-rich vein shows 285.0 eV absorption designed to aromatic carbon and 286.5 eV absorption designed to ketone (C=O), as well as a weak absorption at 288.7 eV assigned to carboxyl/ester [(C=O)O] (Fig. 2). The N-XANES shows absorption at 398.6, 399.7 and 401.1 eV. The 398.6 and 399.7 eV can be attributed to imine/nitrile/pyridine groups, and 401.1 eV can be attributed to amide/pyrrole groups [e.g., 9].

The C-XANES features confirmed that the clast was not subjected to thermal metamorphism in the Carancas H4-5 parent body. The C-XANES of the organic vein is distinguished from that of typical primitive chondritic insoluble organic matter (IOM), and dominated in C=O structures. It indicates that the organic matter is originated in relatively oxygen rich condition. The vein-like morphology indicates that fluid was involved during formation of this structure. Thus the organic vein is formed during aqueous alteration in the clast parent body.

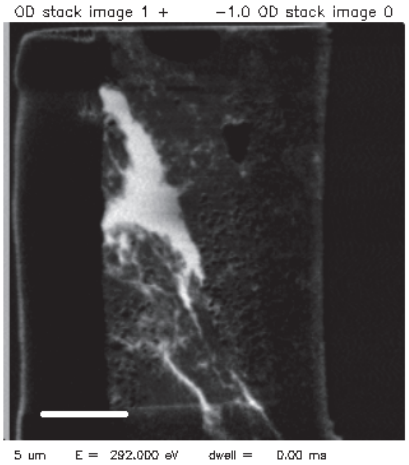

Fig. 1. Carbon map obtained from a FIB section from the clast in the Carancas meteorite. The while area is organic vein-like structure. The map was derived with 292 eV and 280 eV images. The scale bar is 5 μm.

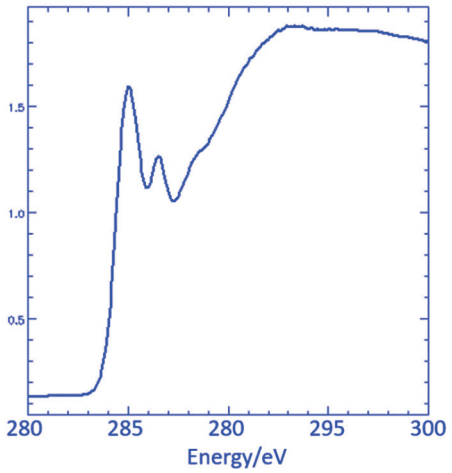

Fig. 2. The C-XANES spectrum obtained from the organic vein in the clast from the Carancas meteorite.

[1] A. J. Brearley, Geochim. Cosmochim. Acta **54** (1990) 831.
[2] M. Zolensky *et al*., Meteoritics **27** (1992) 596.
[3] Y. Kebukawa *et al*., Geochim. Cosmochim. Acta **196** (2017) 74.
[4] Q. H. S. Chan *et al*., Sci. Adv. **4** (2018) eaao3521.
[5] Y. Kebukawa *et al*., Nat. Astro. Submitted.
[6] H. F. Levison *et al*., Nature **460** (2009) 364.
[7] M. Zolensky *et al*., LPSC abst. (2018) 1789.
[8] Q. H. S. Chan *et al*., LPSC abst. (2018) 1191.
[9]P. Leinweber *et al*., J. Synchrotr. rad. **14** (2007) 500.

BL4U

Direct Observation of the Basalt-cell Interface by STXM -Study on the Mechanism of Microbial Alteration of Oceanic Crust-

S. Mitsunobu[1, 2], Y. Ohashi[2] and T. Ohigashi[3]

[1]*Department of Agriculture, Ehime University, Matsuyama 790-8566, Japan*
[2]*Institute for Environmental Sciences, University of Shizuoka, Shizuoka 422-8526, Japan*
[3]*UVSOR Synchrotron Facility, Institute for Molecular Science, Okazaki 444-8585, Japan*

Alteration of oceanic basalts is an important water-rock interaction ubiquitously occurring in the vast oceanic crust. The alteration of oceanic basalt has a significant impact on Earth's climate on a geological timescale by providing a sink for atmospheric CO_2 through carbonization of oceanic basalts (e.g., Standigel et al., 1989; Sleep & Zahnle, 2001). The fresh basalt rock contains abundant Fe (roughly 9 wt.%) and its dominant species is ferrous iron (Fe(II)) and Fe(II)/Fe_{total} ratio in fresh basalt ranges between 82 and 90% [1]. Hence, when the oceanic basalts are exposed to oxidative conditions (e.g., oxygen-saturated seafloor), the Fe(II) in basalts is gradually oxidized to Fe(III) in the alteration process on a geological timescale even at low temperature in deep seafloor [2]. Recent studies have noticed that oceanic microbes (mainly bacteria and archaea) play a significant role to the oxidation of Fe(II) in the basalt. Also, microbial Fe(II) oxidation accelerate the whole alteration process of oceanic crust [2], as the rate of biogenic Fe(II) oxidation is generally more rapid than that of abiotic (chemical) oxidation. There have been considerable efforts to identify mechanisms of the oxidation of Fe(II) involved in the oceanic basalt. However, little is known on the mechanism of microbial Fe(II) in the basalt alteration, because direct chemical speciation of metals and biomolecules at mineral-microbe interface has been difficult due to high spatial resolution in analysis.

Here, we investigated the mechanisms of the Fe(II) oxidation in basalt alteration by scanning transmission X-ray microscopy (STXM) based C and Fe near edge X-ray absorption fine structure (NEXAFS) analyses at UVSOR BL4U. The basalt samples used in the study was the basalt glass samples incubated for 12 months at deep seafloor (the depth of waster: ca. 700 m) in Izu-Ogasawara bonin.

Figure 1 shows the STXM-based merged Fe/C image and C 1s NEXAFS. The C NEXAFS showed that the spectrum measured at bacteria cell-basalt interface in the incubated basalt glass contains a significant peak specific for acidic polysaccharides like alginate, addition to the other biomolecules (protein , DNA, and lipid), and this spectral feature was not found in those of the other area. This finding indicates that the bacteria on the basalt glass produce the polysaccharide-rich extracellular polymeric substances (EPS) at the cell-basalt interface. The biogenic polysaccharides often form a strong complex with Fe ion under wide pH region [3]. Thus, our finding obtained by C NEXAFS analysis imply that observed bacteria could produce the polysaccharides to enhance the dissolution of basalt by the complexation and/or mediate contact between the cell and basalt surface. These findings could be important information for understanding key mechanism of biogenic alteration of ocean crust, basalt.

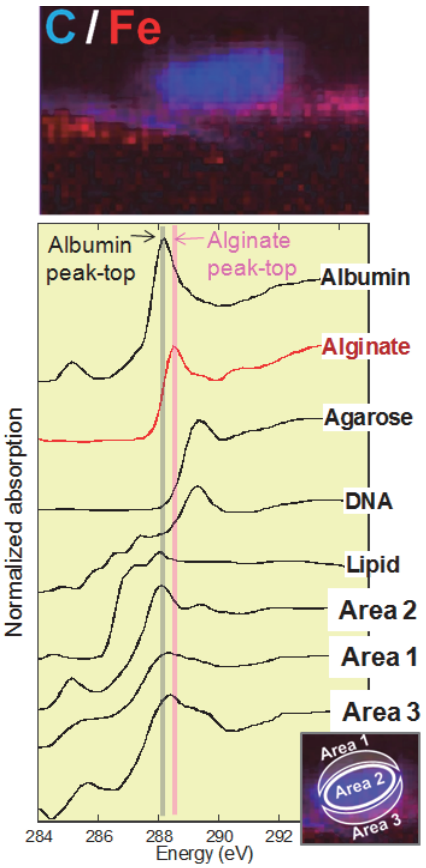

Fig. 1. STXM-based C and Fe images (upper) and C 1s NEXAFS spectra (bottom).

[1] A. Bezos and E. Humler, Geochim. Cosmochim. Acta **69** (2005) 711.
[2] W. Bach and K.J. Edwards, Geochim. Cosmochim. Acta **67** (2003) 3871.
[3] S. Mitsunobu *et al.*, Chem. Lett. **44** (2015) 91.

BL4U

3-Dimensional Observation of a Cell Nucleus by Using a Scanning Transmission X-ray Microscope

T. Ohigashi[1, 2], A. Ito[3], K. Shinohara[3], S. Tone[4], Y. Inagaki[1] and N. Kosugi[1, 2]

[1]*UVSOR Synchrotron Facility, Institute for Molecular Science, Okazaki 444-8585, Japan*

[2]*School of Physical Sciences, The Graduate University for Advanced Studies (SOKENDAI), Okazaki 444-8585, Japan*

[3]*School of Engineering, Tokai University, Hiratsuka, 259−1292, Japan*

[4]*Graduate School of Advanced Science and Technology, Tokyo Denki University, Hatoyama, 350-0394, Japan*

Apoptosis is a process of a programmed cell death observed in many biological processes. Nuclear condensation and DNA fragmentation occur during execution of apoptosis and this process is classified into 3 stages. Generally, apoptosis is observed by using fluorescence microscope with staining process but high resolution image, chemical compositions and 3-dimensional (3D) structure are still unclear. Then, we use a scanning transmission X-ray microscopy (STXM). In these years, we have been developing computed tomography (CT) to perform 3D spectroscopy by changing the energy of the X-ray [1, 2]. By using this technique, 3D distributions of protein and DNA of an isolated cell nucleus were observed.

As the sample preparation, isolated nuclei from HeLa S3 cells were attached on a slide glass using cell adhesive agent, Cell-Tak (Fisher Scientific), and were fixed by glutaraldehyde. After critical point drying process, the isolated cell nucleus was glued on a tip of a tungsten needle. The sample was mounted on a CT sample cell.

Experiment was performed at BL4U. To perform CT, a focal depth of a Fresnel zone plate (FZP) should be longer than thickness of the sample to assume paths of the X-rays through the sample as a parallel beam. Therefore, the FZP with smaller NA was used instead of higher spatial resolution. In this experiment, the FZP with the outermost zone width of 45 nm was used and the focal depth of 5.2 μm at 400 eV is nearly enough length for a cell nucleus.

NEXAFS spectra of DNA and histone as protein around N K-edge are shown in Fig.1. These spectra show remarkable difference on 1s-π* transition so that they were used as reference spectra. In CT measurement, 41 X-ray transmission images (energy stack) were acquired by changing the X-ray energy from 397 to 410 eV. 50 energy stacks were acquired by rotating the sample 3.6° each (180° rotation in total). Then, a size of one image was 8×8 μm^2 with 50×50 pixels and a dwell time was 2 ms per a pixel.

For reconstruction of 3D chemical distributions, the X-ray transmission images of the energy stack were aligned and 2D distributions of DNA and protein were obtained by fitting their reference spectra to each energy stack by using aXis2000 software. Sinograms were extracted from data sets of the 2D distributions of DNA and protein respectively and cross sectional images were reconstructed by home-made filtered back-projection algorithm. The reconstructed 3D distribution of DNA and 2D distributions of DNA and protein are shown in Fig. 2. While the 2D distribution of DNA in Fig. 2(b) shows distinct sub-nuclear structures (shown by arrows), presumably nucleoli, that of protein in Fig. 2(c) shows only the compartment like structures and less protein in the nucleoli.

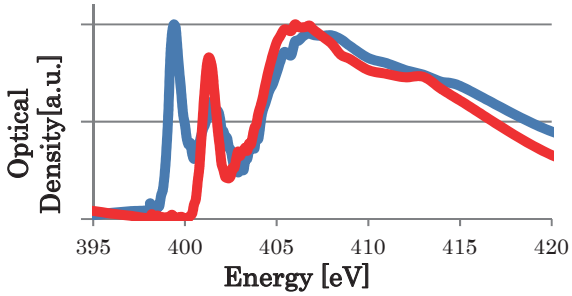

Fig. 1. NEXAFS spectra of DNA (blue) and protein (red) at N K-edge.

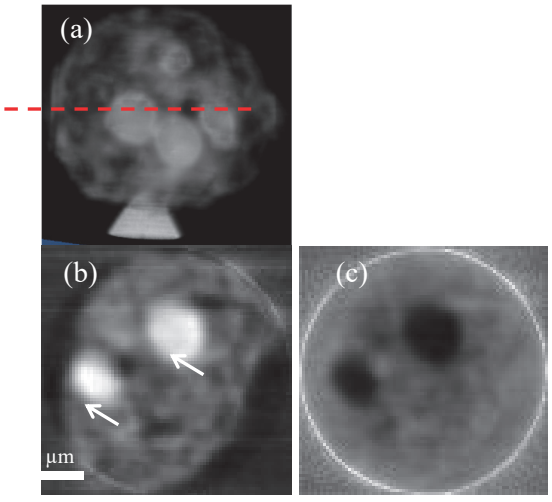

Fig. 2. (a) 3D volume projection image of distribution of DNA and 2D distribution of (b) DNA and (c) protein at the dashed line in (a).

[1] T. Ohigashi, Y. Inagaki, A. Ito, K. Shinohara and N. Kosugi, UVSOR Activity Report **44** (2017) 39.
[2] T. Ohigashi, Y. Inagaki, A. Ito, K. Shinohara and N. Kosugi, J. Phys.: Conf. Ser. **849** (2017) 012044.

BL4U

Investigation of Carbonaceous Materials Inside Moderately Shocked Ureilite Using STXM-XANES System

M. Uesugi[1], T. Ohigashi[2] and Y. Inagaki[2]
[1]*Japan Synchrotron Radiation Research Institute, JASRI, Sayo 679-5198, Japan*
[2] *UVSOR Synchrotron Facility, Institute for Molecular Science, Okazaki 444-8585, Japan, Japan*

Ureilite is a unique class of meteorite which shows small carbonaceous materials inside veins or sometime inclusion like structure, inside the rocky matrix [1-3]. It shows iron-sulfide inclusions or veins, indicating that the meteorite would not come from differentiated asteroids (Fig. 1). On the other hand, silicate materials inside the ureilite shows igneous texture, and their composition is similar to peridotite of Earth, those formed from highly differentiated mantle. On the other hand, oxygen isotopic composition of the ureilite shows close relation with the carbonaceous chondrites, most primitive class of meteorites. In addition, existence of carbonaceous materials also indicates their relation. However, abundance of the carbonaceous materials inside the ureilite is much higher than carbonaceous chondrites, and the carbon material includes euhedral graphite and 100μm-sized diamond inclusions, those rarely found in carbonaceous chondrites. It is interesting that ureilites those showing low impact features do not show diamond inclusions. It might indicate that diamond inclusions inside the carbonaceous material would be formed by heavy shock on the asteroids. However, those carbonaceous material shows noble gas content. It is unlikely that long-heated and highly-shocked materials contain such abundant noble gas. Thus, origin of carbonaceous materials inside the ureilite is still unknown, though it might have important information for the time series of evolution of carbonaceous chondrites.

We investigated Kenna meteorite, a ureiite which shows moderately shocked texture, using x-ray diffraction computed tomography (XRD-CT) at SPring-8, in order to investigate the relation between the shock degree and characteristics of carbonaceous materials. We found that distribution of several different phases of carbonaceous materials inside the meteorite, those are not reported previously.

In this study, we investigated the carbonaceous materials inside Kenna meteorite using scanning transmitted x-ray microscope and x-ray absorption near edge analysis (STXM-XANES), to investigate and identify the phases of carbonaceous materials included inside the meteorite. We lifted up several ultrathin-sections from several points of the meteorite using Focused ion beam (FIB), and investigated the difference of the molecular structure of the carbon phases. Figure 2 shows the result for the STXM-XANES analysis of a thin section of carbonaceous materials picked up from the vein of the meteorite. It shows quite complicated structure of graphite, diamond, amorphous and some unknown phases.

Unfortunately, we could not find the specific phases appeared in the XRD-CT image in this investigation yet. After the analysis of UVSOR, we plan to investigate same sections by transmission electron microscope (TEM) and electron diffraction system, for high resolution analysis.

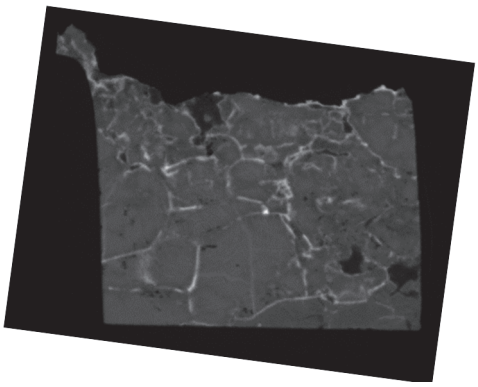

Fig. 1. An X-ray CT image of Kenna meteorite. The with of the sample is 3mm. White veins are iron-sulfide and dark portions are carbonaceous inclusions. Some of veins also includes carbonaceous material.

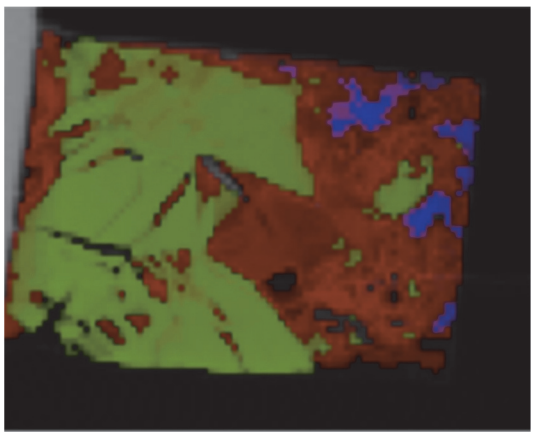

Fig. 2. Mapping of carbonaceous materials. (green: amorphous, red: graphite, blue: diamond, black: unknown). The width of the section is 20 μm.

[1] J. L. Berkley, G. J. Taylor, K. Kell, G. E. Harlow and M. Pnnz, Geochim. Cosmochim. Acta, **44** (1980) 1579.
[2] H. Takeda, Earth Planet. Sci. Lett. **81** (1987) 358.
[3] H. Takeda, Earth Planet. Sci. Lett. **93** (1989) 181.

BL4U

Silica-bearing Minerals in Martian Meteorites

H. Suga[1], N. Shiraishi[1], N. Sago[1], M. Miyahara[1], T. Ohigashi[2], Y. Inagaki[2], A. Yamaguchi[3], N. Tomioka[4], Y. Kodama[5] and E. Ohtani[6]

[1]*Department of Earth and Planetary Systems Science, Graduate School of Science, Hiroshima University, Higashi-Hiroshima 739-8526, Japan*

[2]*UVSOR Synchrotron Facility, Institute for Molecular Science, Okazaki 444-8585, Japan*

[3]*National Institute of Polar Research, Tokyo 190-8518, Japan*

[4]*Kochi Institute for Core Sample Research, Japan Agency for Marine-Earth Science and Technology, Nankoku 783-8502, Japan*

[5]*Marine Works Japan, Nankoku 783-8502, Japan*

[6]*Department of Earth Sciences, Graduate School of Science, Tohoku University, Sendai 980-8578, Japan*

Nakhlite is a unique Martian meteorite clan because it has stark evidence for a rock-fluid reaction occurred on the Mars. Olivine [$(Mg,Fe)_2SiO_4$] occurs in Nakhlite. One of representative evidence for the rock-fluid reaction in Nakhlite is "iddingsite", which is the alteration texture formed in and around the olivine grain. Varied kinds of secondary minerals occur in the iddingsite [e.g., 1]. The mineral species, assemblages, compositions and chemical species of the secondary minerals depend on several parameters such as the temperature and pH of the fluid. Accordingly, Nakhlite allows us to elucidate the physicochemical properties of the fluid existed on ancient Martian surface and its origin. Many previous studies propose that sulfate minerals exist on the Martian surface [e.g., 2]. When sulfate minerals dissolve into solution, sulfate anion and hydrogen ion occur in the solution, which decreases the pH value in the solution. Silica precipitates through the dissolution of olivine under very low pH condition (pH = 0~3); $(Mg,Fe)_2SiO_4 + 4H^+ \rightarrow Si(OH)_4 + 2(Mg,Fe)^{2+}$. Si L_{III}-edge XANES allows us to clarify chemical bonding state around Si [2]. However, Si-XANES was not taken from a natural sample, because the transmittance of the Si L_{III}-edge energy (around 100 eV) is very low. Hence, we attempt to take Si-XANES from the iddingsite in Nakhlite.

Nakhlites, the Yamato (Y) 000593 and Yamato (Y) 000749 were used for this study. Several portions including the iddingsite were extracted by FIB. We prepared the FIB foils having two different thicknesses (Fig. 1). We obtained O-, S- and Fe-XANES from the thick portion, whereas Si- and S-XANES from the thin portion. The foils were observed with TEM/STEM- EDS after STXM analysis.

Laihunite, ferrihydrite, amorphous or poor crystallized silica-rich portion and iron sulfate were identified as a secondary mineral in the iddingsite through TEM/STEM-EDS and STXM analysis. Based on S-XANES, sulfur included in the iron sulfate is hexavalent (Fig. 2(b)). Considering TEM/STEM-EDS analysis and selected area electron diffraction (SAED) patterns, the iron sulfate is natrojarosite [$NaFe_3(SO_4)_2(OH)_6$]. Si L_{III}-edge XANES spectrum were successfully obtained from the poor crystallized silica-rich portion besides montmorillonite and opal as a reference material (Fig. 2(a)). The Si-XANES obtained from the poor crystallized silica-rich portion appears to be montmorillonite (clay mineral: smectite group), which is supported by the SAED patterns. It is likely that the dissolved Si under low pH condition precipitates as clay mineral.

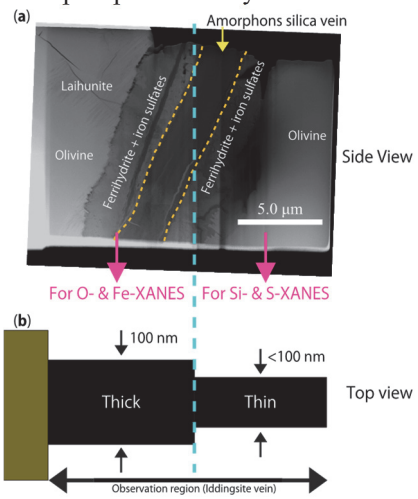

Fig. 1. The FIB foil extracted from the iddingsite in Y 000749. **a**) HAADF-STEM image. The yellow dotted line shows the distribution of the silica-rich portiojn. **b**) A shcematic of crossection of the FIB foil.

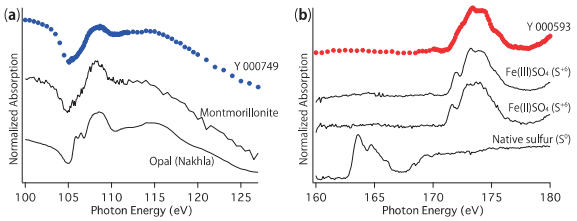

Fig. 2. Representative XANES spectrum. **a**) Si-XANES obtained from the poor crystallized silica-rich portion (blue). Reference spectrum are also shown. **b**) S-XANES obtained from the iron sulfate coexisting with ferrihydrite in Y 000593 (red). Reference spectrum are also shown.

[1] H. Suga *et al.*, Goldschmidt Conference 2017 (2017) 3814pdf.
[2] J. M. Lewis *et al.*, Astrobiology **15** (2015) 247.
[3] L. A. J. Garvie and P. R. Busek, Am. Mineral. **84** (1999) 946.

BL4U

Quantitative Mapping of DNA and Protein in Human Chromosome by Spectromicroscopy with STXM Using Combined NEXAFS Measured at the C, N, and O-K Edges

A. Ito[1], K. Shinohara[1], T. Ohigashi[2, 3], S. Tone[4], M. Kado[5], Y. Inagaki[2] and N. Kosugi[2, 3]

[1]*School of Engineering, Tokai University, Hiratsuka 259-1292, Japan*
[2]*UVSOR Synchrotron Facility, Institute for Molecular Science, Okazaki 444-8585, Japan*
[3] *SOKENDAI (The Graduate University for Advanced Studies), Okazaki 444-8585, Japan*
[4]*Graduate School of Science & Engineering, Tokyo Denki University, Hatoyama 350-0394, Japan*
[5]*Kansai Photon Science Institute, Nat. Inst. Quantum and Radiological Sci. Technol., Kizugawa 619-0215, Japan*

Spectromicroscopy using scanning transmission X-ray microscope (STXM) has been applied to DNA and protein distributions in biological specimens such as chromosome and sperm at the C-K absorption edge [1, 2]. We proposed the use of a unique NEXAFS peak of DNA at the N-K absorption edge for DNA imaging [3], and in our previous study using STXM at BL4U, we obtained DNA and histone, a nuclear protein, distributions in mammalian cells using NEXAFS at the N-K absorption edge [4].

In the present study, to extend the usefulness of the unique DNA peak we developed the procedure for quantitative mapping of DNA, protein and other biomolecules. In addition, the resultant images were compared with the results obtained by the widely used analytical method named as SVD (Singular Value Decomposition).

We used chromosomes for the mapping of DNA, histone and other biomolecules, because they have rather simple molecular composition, DNA and histone. Cultured Chinese Hamster Ovary (CHO) cells were treated with colcemid to stop cell cycle at the beginning of mitotic phase, then mitotic cells that were detached from culture dish were collected and fixed with the mixed solution of ethanol and acetic acid (3:1). The fixed chromosomes were dropped on formvar membrane, and then dried in air. For spectromicroscopy, we measured NEXAFS of DNA, histone, a lipid, phosphatidylcholine (PC), at the C, N, and O-K edges. The image and spectrum analyses were performed using aXis2000 software.

Our procedure to obtain molecular maps is as follows: Images obtained at three absorption edges are combined to form one image stack file. NEXAFS spectra are also combined to form one spectrum. DNA image is obtained by the difference between images on and below the unique DNA peak at the N-K edge. Then DNA stack file is formed by scaling normalized DNA NEXAFS spectrum with the DNA peak height by DNA quantity in each pixel of DNA image. DNA stack file is subtracted from the image stack file. Since the resultant image stack file has no DNA component, the similar procedure can be applied to obtain a stack file of other molecules one by one using possible specific NEXAFS peak for each molecule.

Figure 1 shows chromosome image by STXM at 400 eV. The calculated DNA, histone and PC images are shown in Fig. 2a. The discrete distribution of DNA was observed, which possibly reflects band structure in a chromosome. In Fig. 2b images of the same molecules obtained by SVD method were shown for comparison. The images are not so resolved compared with images by our method, and the molecular contents were largely different (data not shown). SVD method may not be suitable for applying straightly to biological specimens with complex molecular composition.

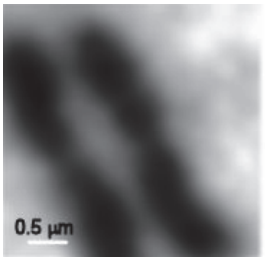

Fig. 1. STXM image of chromosomes of CHO cells at 400 eV.

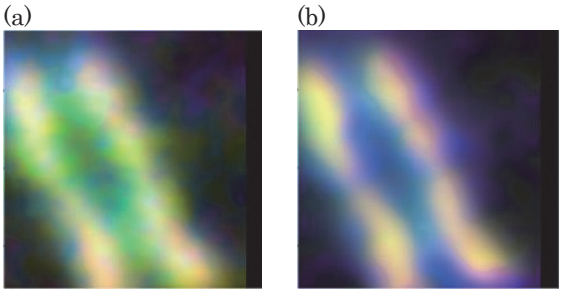

Fig. 2. RGB expression of molecular distribution in chromosomes.
DNA, protein, PC are displayed with red, green and blue, respectively. (a) present method, (b) SVD

[1] H. Ade et al., Science, **258** (1992) 972.
[2] X. Zhang et al., J. Struct. Biol., **116** (1996) 335.
[3] K. Shinohara, A. Ito, K. Kobayashi, In: X-Ray Microscopy and Spectromicroscopy, Springer-Verlag, Berlin/Heidelberg (1998), pp. III-157-III-161.
[4] A. Ito, T. Ohigashi, K. Shinohara, S. Tone, M. Kado, Y. Inagaki and N. Kosugi, UVSOR Activity Report 2015 **43** (2016) 143.

BL4U

Chemical Bonding State Change of Phosphodiester Bonds in Plasmid DNA

T. Ejima[1], T. Ohigashi[2], M. Kado[3] and S. Tone[4]
[1]*IMRAM, Tohoku University, Sendai 980-8577, Japan*
[2]*UVSOR Synchrotron Facility, Institute for Molecular Science, Okazaki 444-8585, Japan*
[3] *Takasaki Adv. Rad. Res. Inst., QST, Takasaki 370-1292, Japan*
[4]*Sch. of Sci & Technol., Tokyo Denki University, Hatoyama 350-0394, Japan*

During the apoptotic process, phosphodiester bonds in DNA are cleaved then DNA strand is broken [1]. When the chemical bonding state change of the phosphodiester bond can be observed according to progress of the DNA cleavage, the DNA cleavage in a cell-nucleus will be visualized by utilizing the chemical bonding state change of the phosphodiester bond. In advance of the visualization of the DNA cleavage, the P-$L_{2,3}$ absorption edge structure of plasmid DNA is investigated, and the results of the edge structures are compared with those of some phosphate materials, such as di-nucleotide, tri-nucleotide, AMP, and cAMP.

Measured samples were a commercially available plasmid DNA that was air-dried as it was on a 50nm thick SiN membrane and that was cleaved with EcoRI and air-dried on a same 50 nm thick SiN membrane. X-ray absorption spectroscopy measurement was made in STXM at BL4U of UVSOR. Energy resolution E/δE was >1000 and spatial resolution was 50 nm. Measured spectra are shown in Fig. 1.

Spectral shapes of measured P - $L_{2,3}$ XAS spectra can be reproduced by 6 peaks, which are indicated by alphabets designated in the figure. Energy positions and peak intensities of corresponding peaks between the spectra are similar to each other except for peak D. Spectral structures of di-nucleotide, tri-nucleotide, AMP, and cAMP show similar shape and are composed of 6 peaks at the same energy range. When the spectral shapes are compared with that of KH_2PO_4 [2], which spectral shape show the six peaks, which spectral shape show the six peaks, the peaks A and B, the peaks C and D, and the peaks E and F will be originated from P3s+O2p, P3p+O2p, and P3d+O2p, respectively.

Peak intensity of peak D will be increased as the result of DNA-cleavage reaction. The comparison of the spectral shapes between the measured spectra and that of KH_2PO_4 suggest that the difference of the DNA cleavage is associated with the P3p+O2p bonds, and that state of DNA cleavage in cell-nucleus may be visualized by the intensity difference of peak D.

This work was supported by Grants-in-Aid for Scientific Research (JSPS Kakenhi, Grant Number: 16H03902 and 17K190210). Prof. K. Shinohara and Prof. A. Ito are thanked for discussions. Y. Inagaki is thanked for assistance of the measurements.

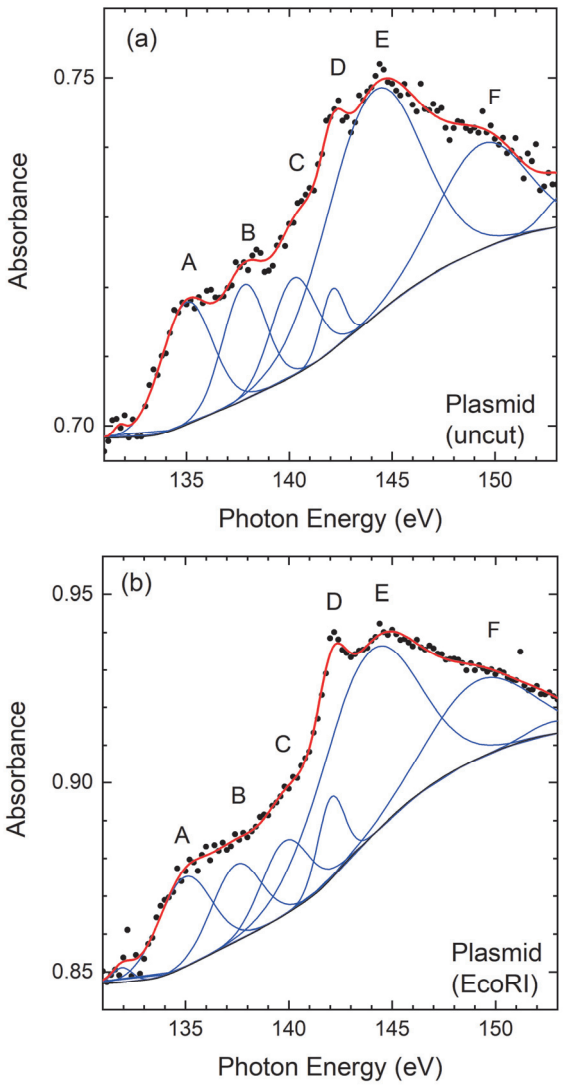

Fig. 1. P-$L_{2,3}$ XAS spectrum of plasmid DNA that air-dried as it is, (a), and that cleaved with EcoRI and air-dried, (b). Dots represent the measurement results, blue curves are deconvolution results, and red cures, the summation of the peaks.

[1] S. Tone *et al*., Exp. Cell Res. **313** (2007) 3635.
[2] S. O. Kucheyev, *et al*., Phys. Rev. B **70** (2004) 245106.

BL4U

Investigation of Origin and Evolution of Extraterrestrial Materials by Visualizing Molecular Structure and Construction of Analytical Scheme with Facility-crossing Collaboration of Hayabusa2 Retuned Samples

M. Uesugi[1], M. Ito[2], N. Tomioka[2], K. Uesugi[1], A. Yamaguchi[3], N. Imae[3], T. Ohigashi[4], N. Shirai[5], Y. Karouji[6], T. Yada[6], M. Abe[6] and Y. Inagaki[4]

[1]*Japan Synchrotron Radiation Research Institute (JASRI/SPring-8), Sayo 679-5198, Japan*
[2]*Japan Agency for Marine-Earth Science and Technology (JAMSTEC), Nankoku 783-8502, Japan*
[3]*National Institute of Polar Research (NIPR), Tachikawa 190-0014, Japan*
[4]*UVSOR Synchrotron Facility, Institute for Molecular Science (IMS), Okazaki 444-8585, Japan*
[5]*Tokyo Metropolitan University, Hachioji 192-0364, Japan*
[6]*Japan Aerospace Exploration Agency (JAXA), Sagamihara 252-5210, Japan*

Extraterrestrial sample curation center (ESCuC) of Japan aerospace exploration agency (JAXA) organized a special team for the development of techniques and devices for the handling, transfer and analysis of samples returned by Hayabusa2 spacecraft, from 2015 under the agreements of collaboration. The special team constitutes of members of institutes those having state-of-the-art analytical instruments and experiences of curatorial works of precious natural samples, but beyond the specialists of the extraterrestrial materials [1-2].

We started development of new analytical protocols of extraterrestrial materials, which includes method of sample transfer, sample separation and data sharing, through the rehearsals of the curation works for the initial description of Hayabusa2-returned samples using extraterrestrial materials. Currently, 5 Antarctic micrometeorites (AMMs) provided by national institute of polar research (NIPR) were imaged by synchrotron radiation computed tomography (SR-CT) and x-ray diffraction (XRD) at SPring-8, and investigated by high resolution field emission scanning electron microscopy and energy dispersive spectroscopy (FE-SEM-EDS) system at institute for molecular sciences (IMS) (Fig. 1). Through the series of non-destructive analysis, we selected Antarctic micrometeorites those having similar characteristics of carbonaceous chondrites.

In this study, we formed thin sections of two AMMs selected by the results of non-destructive analyses, using focused ion beam (FIB) for the characterization of organic materials by scanning transmitted x-ray microscopy and x-ray absorption near edge structure analysis (STXM-XANES) at BL4U. One section for a fragment of AMM, TT006cT0009-1-1 was analyzed by nano-scale secondary ion mass spectrometry (NanoSIMS) before the STXM-XANES, and obtained isotopic mapping images of the light elements such as hydrogen, carbon, nitrogen and oxygen by at Japan agency for marine-earth science and technology (JAMSTEC). After NanoSIMS analysis, the section was fabricated by FIB again, to make ultrathin section for the STXM-XANES analysis. Other sections were prepared without NanoSIMS analysis.

Figure 2 shows STXM image of TT006cT0009-2-1 obtained using a NanoAnalysis linkage grid (Kochi grid) developed in our activity. We could safely prepare the sample in atmosphere shielding environment using glovebox and sample loading system equipped at BL4U, and investigated the ultrathin-section without paper tape. Further result of our analyses will be reported by subsequent papers (in prep).

After the STXM-XANES analysis, the ultrathin-sections will be analyzed by transmission electron microscopy (TEM), for high resolution analysis of nano-scale textures and crystal structures inside the AMMs.

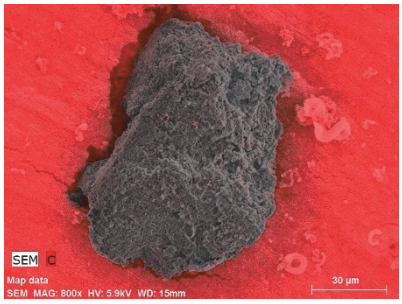

Fig. 1. An energy dispersion spectroscopy image of TT006cT0009-2. Red shows carbon distribution.

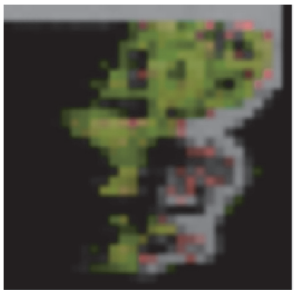

Fig. 2. A STXM-XANES image of a ultrathin-section of TT 006cT0009-2. Green portion shows region enriched in graphene, and red portion shows region enriched in carboxyl and poor in graphene.

[1] M. Uesugi *et al.* Abstract Haybusa symp. (2016) #1129
[2] M. Uesugi *et al.* Abstract Haybusa symp. (2017) #1129

BL4U

Probing the Penetration of Tofacitinib and Tofacitinib Citrate in Inflamed Murine Skin by Soft X-Ray Spectromicroscopy

K. Yamamoto[1], A. Klossek[1], J. Berkemeyer[1], T. Ohigashi[2], F. Rancan[3], R. Flesch[1], A. Vogt[3], U. Blume-Peytavi[3], M. Radbruch[4], H. Pischon[4], A. D. Gruber[4], L. Mundhenk[4], N. Kosugi[2] and E. Rühl[1]

[1]*Institute for Chemistry and Biochemistry, Freie Universität Berlin, Takustr. 3, 14195 Berlin, Germany*
[2]*UVSOR Synchrotron Facility, Institute for Molecular Science, Okazaki 444-8585, Japan*
[3]*Charité Universitätsmedizin, 10117 Berlin, Germany*
[4]*Veterinary Pathology, Freie Universität Berlin, 14163 Berlin, Germany*

The penetration of hydrophilic and hydrophobic drugs into human skin is systematically investigated by label-free detection employing soft X-ray microscopy. The FDA-approved anti-inflammatory drug tofacitinib citrate ($C_{16}H_{20}N_6O \cdot C_6H_8O_7$, molecular weight 504.49 g/mol), marketed under the name Xeljanz, is chosen as a hydrophilic drug, which acts as a JAK inhibitor by interfering with the JAKSTAT signaling pathway. It is a low molecular weight drug that is commonly used for oral drug delivery for treating e.g. rheumatoid arthritis. Its use for treating plaque psoriasis is currently under investigation [1]. We also included the free base of tofacitinib ($C_{16}H_{20}N_6O$, molecular weight 312.37 g/mol) as a hydrophobic complement to tofacitinib citrate. This enables us to investigate the influence of hydrophilicity on dermal drug penetration.

The experiments made use of excised murine skin, which was inflamed and exposed to tofacitinib citrate and the free base obtained from LC Labs for penetration times between 10 and 1000 min, similar to earlier work using dexamethasone as a drug [2-3].

Spectromicroscopy studies were performed at the BL4U at UVSOR III using a scanning X-ray microscope. The chemical selectivity for probing the drugs in EPON-fixed skin was achieved by exciting the samples selectively at the O 1s-edge in the pre-edge regime, i.e. at 528 eV (pre-edge) and 531.8 eV, respectively, corresponding to the O 1s→ π* transition of the drugs. Figure 1 shows the O 1s regime of fixed murine skin, tofacitinib, and tofacitinib citrate.

Figure 1. This provides chemical selectivity for label-free probing of tofacitinib. Differential absorption maps corresponding to the drug distribution as a function of depth were derived similar to our previous work [2-3]. Figure 2 shows the drug distribution in the top skin layers, consisting of stratum corneum (SC) and viable epidermis (VE). There are distinct differences between the drug distributions after 100 min penetration time. The hydrophilic drug tofacitinib citrate is primarily found in the top layers of the stratum corneum and no drug is found in deeper skin layers (see Fig. 2(a)). In contrast, the free base is found in deeper layers of the stratum corneum and in the viable epidermis (see Fig. 2(b)). There, the drug is preferably found in the thin membranes of the keratinocytes surrounding the cell nuclei. This corresponds to the site of action of this drug. The present results also indicate that topically applied hydrophobic drugs can more efficiently penetrate the top layers of skin than the hydrophilic analogue.

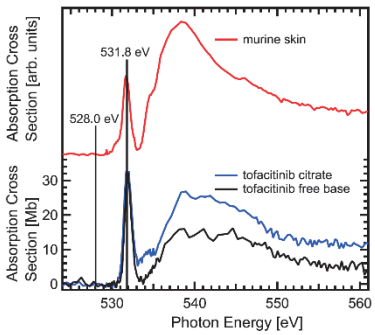

Fig. 1. X-ray absorption of tofacitinib citrate, the free base, and fixed murine skin near the O 1s-edge.

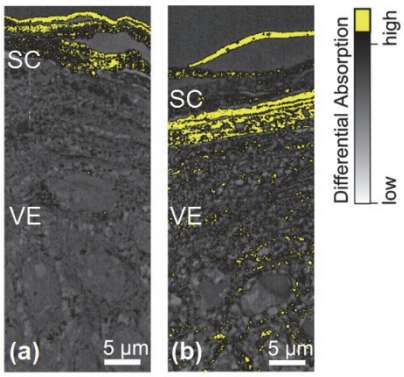

Fig. 2. Differential absorption of (a) tofacitinib citrate and (b) the free base of tofacitinib penetrating the top skin layers of murine skin for 100 min, respectively. High drug concentration is indicated by yellow color.

[1] V. Di Lernia *et al.*, Drug Design Develop. Therap. **10** (2015) 533.
[2] K. Yamamoto *et al.*, Anal. Chem. **87** (2015) 6173.
[3] K. Yamamoto *et al.*, Eur. J. Pharm. Biopharm. **118** (2017) 30.

BL4U

Chemical Mapping Individual Atmospheric Nanoparticles

X. Kong[1*], M. Huttula[1], J. J. Lin[1], P. Corral Arroyo[2], T. Ohigashi[3], N. Kosugi[3, 4], Z. Wu[5] and N. L. Prisle[1]

[1]*Nano and Molecular Systems Research Unit, University of Oulu, Oulu 90041, Finland*
[2]*Laboratory of Environmental Chemistry, Paul Scherrer Institute, CH-5232 Villigen PSI, Switzerland*
[3]*UVSOR Synchrotron Facility, Institute for Molecular Science, Okazaki 444-8585, Japan*
[4]*School of Physical Sciences, The Graduate University for Advanced Studies, Okazaki 444-8585, Japan*
[5]*State Key Joint Laboratory of Environmental Simulation and Pollution Control, College of Environmental Sciences and Engineering, Peking University, 100871, China*
[*]*now at Department of Chemistry and Molecular Biology, University of Gothenburg, Gothenburg, Sweden*

During the STXM beamtime, chemical maps were drawn for two laboratory-generated aerosol samples and one ambient urban aerosol sample.

The laboratory-generated aerosols were produced by the atomization of solutions of sodium n-decanoate and sodium chloride. Particles of 150, 200, and 300 nm were generated from solutions with 0.5 and 0.8 mass fraction of sodium n-decanoate and particles of 30, 50, 80 nm, and polydisperse samples were generated from solutions of 0.25 mass fraction of sodium n-decanoate.

The urban aerosol samples were collected from October 2017 to January 2018 in a winter campaign jointly operated by Peking University and the University of Gothenburg. Sampling was carried out at the Peking University Atmosphere Environment Monitoring Station on the roof of a six-floor building on the campus of Peking University located in the northwestern urban area of Beijing. A SKC 4-stage cascade impactor was used to collect particles with cut-off sizes of 250 and 500 nm that were impacted onto Formvar films.

The urban aerosol samples were examined at the adsorption edges of carbon, nitrogen, sulfur, silicon, chlorine, and potassium. Figure 1 shows the optical density of a particle at the carbon and nitrogen edges. At 284.5 eV, the C=C double bond is shown as the bright area [1], which indicates two soot components located at the two poles of the particle. The spatial resolution of the image is 30 nm. The detailed carbon edge spectrum indicates that the soot particles are well aged. In addition, the potassium L-edge indicates that K^+ ions are present and located in the area between the soot particles. The absorption maxima of the ammonium functional group are around 401 eV, and according to the panel (b) the NH_4^+ mainly stays between the soot particles, like K^+. From panel (c) it seems that the NO_3^- is spread all over the particle. Further quantitative analysis will be performed to calculate the mixing ratio.

The carbon edge adsorption spectrum contains rich information about the functional groups and the oxidation states. Figure 2 shows (a) the carbon spectra of aged soot particles at the carbon edge from 280 eV to 320 eV, where the spectra of different colors are taken from different places of the particle, but they are very consistent except for the amplitudes that is correlated to the particle thickness of the examined regions. Panel (b) shows the spectra of laboratory- generated soot coated by α-pinene (in red) and naphthalene SOA (in black) from literature [2], where the featured peaks excellently match the sampled particle shown in panel (a). The STXM method at BL4U seems to be perfectly suited for the study of both ambient and laboratory nanoparticles.

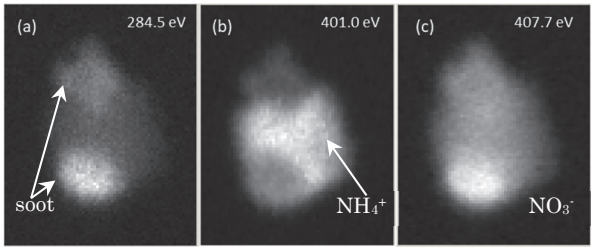

Fig. 1. Optical density at various photon energies. The bright areas indicate where the excited functional groups are located. (a) soot; (b) NH_4^+; (c) NO_3^-.

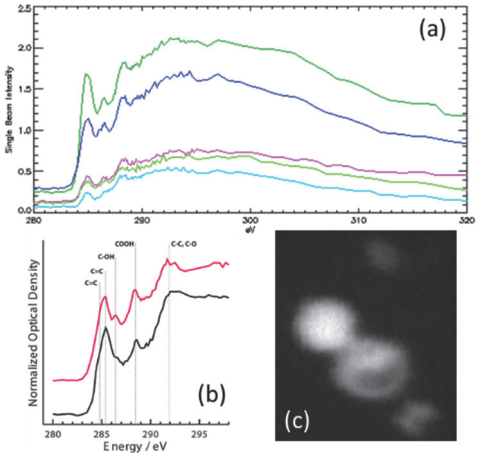

Fig. 2. (a) carbon K-edge adsorption spectra of sampled urban particles; (b) STXM spectra of laboratory-generated soot coated by α-pinene (red) and naphthalene SOA (black) [2]; (c) STXM image of the particles at 286.6 eV.

[1] R. C. Moffet, A.V. Tivanski and M.K. Gilles, "Fundamentals and Applications in Aerosol Spectroscopy" (CRC Press; Boca Raton, Fl, 2011).
[2] J. C. Charnawskas *et al.*, Faraday Discussions, **200** (2017) 165.

BL4U

STXM Studies of Abnormal Ultrastructural Features in FINCA Disease

E.-V. Immonen[1, 2], T. Ohigashi[3], I. Miinalainen[4], M. Patanen[1], R. Hinttala[2, 4], J. Uusimaa[2, 4], N. Kosugi[3] and M. Huttula[1]

[1]*Nano and Molecular Systems research unit, P.O. Box 3000, 90014 University of Oulu, Finland*
[2]*PEDEGO Research Unit and Medical Research Center Oulu, University of Oulu and Oulu University Hospital, PO Box 5000, 90014 University of Oulu, Finland*
[3]*UVSOR Synchrotron Facility, Institute for Molecular Science, Okazaki 444-8585, Japan*
[4] *Biocenter Oulu, PO Box 5000, 90014 University of Oulu, Finland*

In this work, we have used scanning transmission X-ray imaging technique at BL4U to study human tissue samples exhibiting abnormal ultrastructural features related to FINCA disease. Recently, a novel, fatal cerebropulmonary disease in children was characterized with fibrosis, neuro- degeneration and cerebral angiomatosis (FINCA disease) [1]. The disease course is progressive with multiorgan manifestations, leading to death before the age of two years. Studies on autopsy samples revealed interstitial fibrosis and previously undescribed granuloma-like lesions in the lungs, and hepatomegaly related to widespread microvacuolar hepatocyte fatty degeneration and hepatocellular necrosis. All patients had a combination of mutations in the *NHLRC2* gene encoding an NHL repeat containing protein 2 that is ubiquitously present in various types of tissues, from animals to bacteria. Still, no published results exist on the functional role of the NHLRC2.

In order to learn more about the pathomechanism behind FINCA disease, multidisciplinary approaches are called for. These, among others, include morphological and chemical analysis of the subcellular features in the liver autopsy samples taken from the FINCA patients. However, conventional imaging techniques, such as electron microscopy, possess severe pitfalls when it comes to chemical imaging, requiring the utilization of the STXM method. Thus, we have performed the first proof-of-principle STXM studies on subcellular structural characteristics related to storage diseases.

The samples (approximately 150-200 nm thick) were prepared at Biocenter Oulu, Finland using standard methods in transmission electron microscopy (TEM), and placed on Butvar film coated copper grids. In addition, sections adjacent to ones selected for STXM imaging were imaged using TEM, allowing the comparison of these methods as shown in Fig. 1.

The measurements concentrated on C 1s edge, and we have observed several abnormal ultrastructural features in various tissues of a FINCA patient. Figure 1 shows an example of a liver sample, where these abnormal features include large vacuoles of unknown origin (marked as U in Fig. 1). According to carbon K-edge absorption profile, these vacuoles have a chemical signature that differs from other organelles (Fig. 1C). Further studies will focus on verifying the origin and identifying the accumulated compounds. This can be useful in finding novel biomarkers in future for example storage diseases.

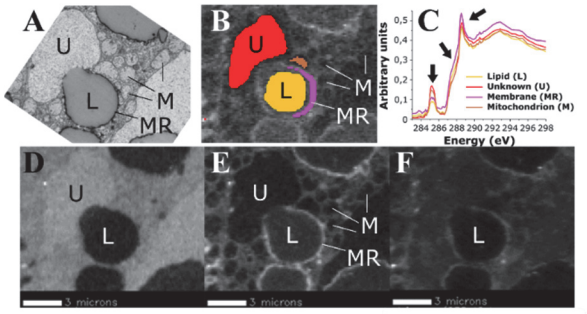

Fig. 1. A) A TEM image showing organelles (lipid vesicles L, their membrane MR, mitochondria M, and an unknown structure U, within a hepatocyte. B) An STXM image of the same region with hν = 287 eV. Subcellular features used for collecting region specific absorption spectra are marked with colors. C) Absorption spectra from regions in B. The arrows indicate the most prominent spectral differences. D) STXM image stack from an energy range 285-286 eV (1st arrow in C). E) Energy range 286-288 eV (2nd arrow in C). F) 288-297 (3rd arrow in C).

[1] J. Uusimaa, R. Kaarteenaho, T. Paakkola, H. Tuominen, M. K. Karjalainen, J. Nadaf, T. Varilo, M. Uusi-Mäkelä, M. Suo-Palosaari, I. Pietilä, A. E. Hiltunen, L. Ruddock, H. Alanen, E. Biterova, I. Miinalainen, A. Salminen, R. Soininen, A. Manninen, R. Sormunen, M. Kaakinen, R. Vuolteenaho, R. Herva, P. Vieira, T. Dunder, H. Kokkonen, J. S. Moilanen, H. Rantala, L. M. Nogee, J. Majewski, M. Rämet, M. Hallman, R. Hinttala, Acta Neuropathol. (2018). In press. https://doi.org/10.1007/s00401-018-1817-z

UVSOR User 7